Biochimica et Biophysica Acta 1838 (2014) 2350–2356

Contents lists available at ScienceDirect

Biochimica et Biophysica Acta

journal homepage: www.elsevier.com/locate/bbamem

Glutamate provides a key structural contact between reticulon-4 (Nogo-66) and phosphocholine ☆

Ali Alhoshani [a], Rosemarie Vithayathil [b], Jonathan Bandong [b], Katherine M. Chrunyk [b], Gabriel O. Moreno [b], Gregory A. Weiss [b,c], Melanie J. Cocco [a,b,*]

[a] Department of Pharmaceutical Sciences, University of California, Irvine, CA 92697, USA
[b] Department of Molecular Biology and Biochemistry, University of California, Irvine, CA 92697, USA
[c] Department of Chemistry, University of California, Irvine, CA 92697, USA

ARTICLE INFO

Article history:
Received 26 February 2014
Received in revised form 9 May 2014
Accepted 16 May 2014
Available online 24 May 2014

Keywords:
Reticulon
Nogo-66
Membrane interface
Structure
Choline
Glutamate

ABSTRACT

Human reticulon 4 (RTN-4) has been identified as the neurite outgrowth inhibitor (Nogo). This protein contains a span of 66 amino acids (Nogo-66) flanked by two membrane helices at the C-terminus. We previously determined the NMR structure of Nogo-66 in a native-like environment and defined the regions of Nogo-66 expected to be membrane embedded. We hypothesize that aromatic groups and a negative charge hyperconserved among RTNs (Glu26) drive the remarkably strong association of Nogo-66 with a phosphocholine surface. Glu26 is an isolated charge with no counter-ion provided by nearby protein groups. We modeled the docking of dodecylphosphocholine (DPC) with Nogo-66 and found that a lipid choline group could form a stable salt bridge with Glu26 and serve as a membrane anchor point. To test the role of the Glu26 anion in binding choline, we mutated this residue to alanine and assessed the structural consequences, the association with lipid and the affinity for the Nogo receptor. In an aqueous environment, Nogo-66 Glu26Ala is more helical than WT and binds the Nogo receptor with higher affinity. Thus, we can conclude that in the absence of a neutralizing positive charge provided by lipid, the glutamate anion is destabilizing to the Nogo-66 fold. Although the Nogo-66 Glu26Ala free energy of transfer from water into lipid is similar to that of WT, NMR data reveal a dramatic loss of tertiary structure for the mutant in DPC micelles. These data show that Glu26 has a key role in defining the structure of Nogo-66 on a phosphocholine surface. This article is part of a special issue entitled: Interfacially Active Peptides and Proteins. Guest Editors: William C. Wimley and Kalina Hristova.

1. Introduction

Reticulons (RTNs) are membrane proteins found in the endoplasmic reticulum (ER) of most eukaryotes. It has been proposed that RTNs evolved when the endomembrane system developed ~1.7 billion years ago [1]. RTNs function to establish curvature of the ER membrane [2] and have been implicated in the assembly of the nuclear envelope [3], ER-Golgi trafficking and vesicle formation (reviewed in [4]). Some viruses exploit the ability of host RTNs to drive lipid bilayers into membrane compartments, enabling the virus to sequester viral replication behind a host membrane (reviewed in [5]). In addition to defining the architecture and topology of a lipid membrane, RTNs have been adapted for other cellular functions including: the regulation of apoptosis [6,7], inhibition of β-amyloid-converting enzyme 1 (BACE1) to block amyloid formation [8,9], vascular remodeling [10], inhibition of angiogenesis in the CNS [11], and inhibition of myelination [12]; and as an axonal growth inhibitor, RTN-4 limits plasticity in the brain (reviewed in [13,14]). RTNs have also been implicated in a range of neurodegenerative diseases (reviewed in [15]). The C-terminal 150–200 amino acids are common among all RTNs and are referred to as the reticulon homology domain (RHD). RHDs have two hydrophobic membrane-embedded regions (Fig. 1B); between these helices is a span of 66 amino acids (RHD-66) that extends beyond the membrane into the aqueous phase. The N-terminal regions of RTNs can vary dramatically in length and sequence, according to their distinct function.

RTN-4 is also known as the neurite outgrowth inhibitor (Nogo). Nogo is expressed as three isoforms: Nogo-A, -B and -C splice variants result in different N-terminal sequences; these can traffic from the ER to the plasma membrane. All Nogo variants share a common C-terminal domain RHD, which includes the 66-residue extracellular region (Nogo-66) [16–18]. Nogo-66 has been identified as one of several

Abbreviations: BACE1, β-amyloid-converting enzyme 1; CNS, central nervous system; CRP, human C-reactive protein; f_p, fraction of protein in lipid phase; DMPC, 1,2-dimyristoyl-*sn*-glycero-3-phosphocholine; DPC, dodecylphosphocholine; ELISA, enzyme-linked immunosorbent assay; HSQC, heteronuclear Single Quantum Correlation spectroscopy; K_x, partition coefficient; NOE, nuclear Overhauser effect; Nogo, neurite outgrowth inhibitor, RTN-4; Nogo-66, 66-residue extracellular region of Nogo; NgR, Nogo receptor; PC, phosphocholine; PfPMT, phosphoethanolamine methyltransferase; RHD, reticulon homology domain; RHD-66, 66-residue extracellular region of an RHD; RTN, reticulon

☆ This article is part of a special issue entitled: Interfacially Active Peptides and Proteins. Guest Editors: William C. Wimley and Kalina Hristova.

* Corresponding author at: 1218 Natural Sciences I, Dept of Molecular Biology and Biochemistry, University of California, Irvine, CA 92697-3900, USA. Tel.: +1 949 824 4487.
E-mail address: mcocco@uci.edu (M.J. Cocco).

http://dx.doi.org/10.1016/j.bbamem.2014.05.021
0005-2736/

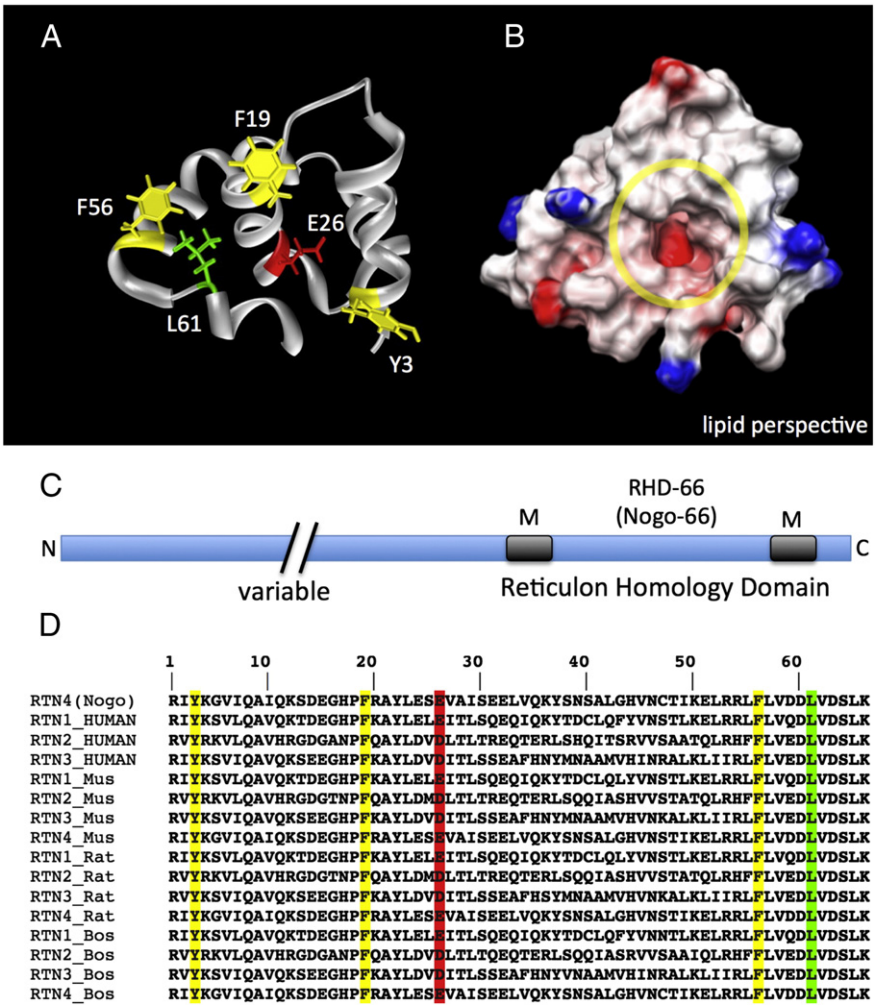

Fig. 1. Structure and homology of Nogo-66. A) Ribbon diagram of Nogo-66 showing the lipid–protein interface of Nogo-66 (PDB ID: 2KO2); groups conserved among higher vertebrate RHDs are highlighted (yellow: Y3, F19, F56; green: L61); a negative charge is hyperconserved (E or D) among all RHDs at position 26 (red: E26). B) surface representation of Nogo66 colored according to electrostatic potential; facing the phosphocholine surface, E26 is visible at the base of a cavity (yellow circle) with no protein counter ion nearby. C) RTN domain organization; the N-terminus varies in length, sequence and function; M = membrane embedded. D) Sequence alignment of RHD-66 (extracellular region) of selected higher vertebrates; conserved groups that contact lipid (featured in A and B) are highlighted.

domains involved in axonal regrowth inhibition [17] and mediates its inhibitory activity by binding to the Nogo receptor (NgR) [19].

Recently, we determined the NMR structure of Nogo-66 embedded in a native-like environment [20]. Nogo-66 is disordered in an aqueous environment, but folds into a five-helix bundle in dodecylphosphocholine (DPC). We used accessibility to paramagnetic reagents and nuclear Overhauser effects (NOEs) between protein and DPC to define the regions of Nogo-66 that are either in contact with DPC or exposed to the aqueous phase, this enabled us to orient the protein. In early functional assays, the peptide corresponding to residues 31–55 of Nogo-66 was found to have the most activity in blocking neuronal growth [17]. The residues that are the most solvent exposed amino acids in our model of Nogo-66 at the cell surface are also most active in binding NgR.

The function of Nogo as an axonal growth inhibitor has been well established (reviewed in [13]), but the structural mechanisms by which RTNs establish membrane curvature remains undefined. Although RTNs can have disparate functions, RHDs share a common function in the ER. Specific contacts between the RHD and lipid and the dominant forces that enable the RHD to establish membrane curvature are currently unknown. We evaluated amino acids that are conserved among all RHDs and developed a list of groups that could be important in lipid interactions. In Nogo-66, we found several positions conserved in higher vertebrates that are in contact with lipid including aromatic and hydrophobic side chains. The position, E/D26 in the 66-amino acid domain was identified as hyperconserved in RTNs of all eukaryotes in 2003 [1]. Furthermore, the structure surrounding Glu-26 is interesting because the side chain is positioned at the base of a cavity that could easily accommodate a phosphocholine (PC) with no positively charged protein groups in proximity to neutralize the Glu carboxylate. The distances between Glu26 and the Lys or Arg side chains of helix 1 and 5 make it impossible for direct interaction, but collectively or individually these groups could form salt bridges to bind the choline and phosphate of a PC molecule. We propose a model for the interaction of a single PC with Nogo-66. Here we explore the structural role of Glu26 and find that interactions between Glu26 and the PC surface of a micelle or lipid vesicle influence the Nogo-66 structure. Moreover, mutation of Glu26 to Ala has structural consequences resulting in increased helical content in aqueous solution, consistent with Glu26 destabilizing the fold when unpaired with choline. Conversely, E26A shows significantly decreased order and helical content in a membrane-like environment revealing the role that this Glu plays in defining the Nogo-66 structure at the membrane surface.

2. Materials and methods

2.1. Nogo-66 protein expression and purification

A plasmid containing WT Nogo-66 has previously been described [20]. The E26A mutant plasmid was prepared using quick-change

mutagenesis (Strategene) and confirmed by DNA sequencing. Proteins were expressed with an N-terminal His_6 tag and six additional amino acids (MHHHHHHLVPRGM). The protein was expressed as described previously. SDS-PAGE and MALDI mass spectrometry confirmed purified protein to be the correct molecular weight. Protein NMR samples were prepared by dissolving lyophilized protein in 5 mM sodium acetate to a final concentration of 1 mM. DPC (Avanti Polar Lipids, Inc.) was added to a final concentration of 200 mM.

2.2. CD measurements

The secondary structure of Nogo-66 was analyzed by CD spectroscopy in the far UV (185–250 nm) regions. Solutions of the protein were dialyzed against 5 mM sodium acetate, pH 5.0. We choose pH 5 to balance Nogo-66 solubility with maintaining the Glu side chain above the pKa. We also collected data at pH 7 at a lower protein concentration and found the same spectral features. 1.9 mg/ml WT and 1.3 mg/ml E26A Nogo-66 samples were analyzed at 25 °C, in 1.0 nm wavelength intervals using a JASCO Model 720 CD spectropolarimeter (JASCO, Easton, MD) with a scan speed of 50 nm/min and average response time of 5 s. A total of 10 consecutive scans were accumulated for analysis. To minimize light scattering inherent in lipid vesicles samples, data were collected with a 0.1-mm path-length cell (NSG Precision Cells, Inc., Farmingdale, NY). DichroWeb, an online server providing various CD analysis programs, was used to analyze the data [21]. The program ContinLL was used to fit the data and estimate the content of secondary structure present using reference set SP175 [22].

2.3. Lipid partitioning assays

To determine the partition coefficient for the transfer of Nogo-66 WT and E26A from water into lipid, CD wavelength spectra were collected at varying lipid concentrations and the change in ellipticity at 222 nm (θ, mdeg) was analyzed as described in [23]. 1,2-dimyristoyl-*sn*-glycero-3-phosphocholine (DMPC) vesicles were extruded to 100 nm diameter particles at 35 °C. Protein and lipid were diluted into separate tubes to maintain a final protein concentration of approximately 0.5 mg/ml, 5 mM sodium acetate, pH 5.0 with varying concentration of lipid (0.01–10 mM). CD spectra were collected at 25 °C The fraction of protein partitioned into the lipid phase (f_p) plotted as a function of lipid concentration was fit to the following equation to determine the partition coefficient, K_X.

$$f_p = \frac{K_X[L]}{[W] + K_X[L]} \tag{1}$$

where [W] is the concentration of water and [L] is the concentration of lipid.

The free energy of transfer from water into lipid bilayer was calculated from the equation:

$$\Delta G = -RT \ln K_X. \tag{2}$$

2.4. NMR measurements

NMR experiments were performed on a Varian Inova 800 MHz NMR spectrometer equipped with a 5 mm xyz, pulse-field gradient triple resonance probe. ^{15}N-HSQC experiments were performed each at a protein concentration of 1 mM WT (pH 4.0) and E26A (pH 4.5) Nogo-66 in presence of 200 mM DPC at 35 °C, in 5 mM sodium acetate, 90% H_2O/10%D_2O. Data were processed using NMRPipe [24].

2.5. Cloning and expression of NgR

The protocol for production of the receptor, NgR was adapted from a previously described report [25] A pCRII-TOPO (Invitrogen) vector for expression in mammalian cell culture, containing mouse Nogo receptor was provided to us by Dr. Binhai Zheng (UCSD). The sequence of NgR was verified and the Nogo ligand binding domain (residues 26–310) was PCR amplified before subcloning into Pharmingen's pAcGp67A secretion vector, which was designed to produce a His_6 tag fused to the C-terminus of NgR. The glycosylated, folded material was successfully produced in Sf9 insect cells (Novagen), which were grown in BacVector Insect cell Media (Novagen) as suspension cultures in a spinner flask at 28 °C. The culture was infected with recombinant baculovirus at a cell density of 1×10^6 cells/ml. The MOI (multiplicity of infection) determined for optimal expression was 5 pfu/ml, and the optimal period of infection was 96 h. Cells were sedimented and the media supernatant with secreted NgR was concentrated 10-fold. Nickel resin was added to the concentrated media, and the standard protocol described by Qiagen for purification of His_6 tag proteins under native conditions was used. The receptor was dialyzed into HBS buffer (HEPES buffered saline pH 7.2, 5 mM Hepes), and concentrated to 2–3 mg/ml.

2.6. Receptor binding assay

The phage-Nogo-66 vector has been described previously [26]. The mutation E26A was made using QuikChange mutagenesis, and the mutation confirmed by DNA sequencing. Phage production and isolation has been described [26]. A phage-based ELISA was used to assess display levels of WT Nogo-66 on the surface of the M13-KO7$^+$ phage by immobilizing an anti-FLAG antibody on the ELISA plate. Followed phage-based ELISA protocol as described in [26]. A single microtiter plate was used to assay simultaneously the display levels (A^0) as well as binding (A) of Nogo-66 wild-type and variant to immobilized NgR. The ratio (A/A^0) represents the apparent binding affinity, K_A:

$$K_A = \frac{A}{A^0} \tag{3}$$

where

A^0 = The absorbances measured in wells coated with AntiFlag antibody. This value quantifies display levels of Nogo-66 wild-type and variant on the phage surface.

A = The absorbances measured in wells coated with NgR. This value quantifies binding levels of Nogo-66 wild-type and variant to NgR [27].

3. Results

Previously, we found that Nogo-66 was disordered in solution but folded into a structure that was 85% helical in the presence of DMPC vesicles [20]. Thus, the structure of Nogo-66 is driven by lipid interactions. To develop a list of potential protein/lipid interactions that could contribute in defining the protein fold, we mapped conserved positions onto the Nogo-66 structure. RTN sequences include one position that is hyperconserved among all RHDs (Fig. 1D red highlight) and other groups that are conserved within the RTNs of higher vertebrates (*e.g.*, Fig. 1D yellow, green highlight) [1]. The positions of proposed lipid-interacting groups conserved in higher vertebrates (Tyr3, Phe19, Phe56, Leu61) and the hyperconserved Glu26 are depicted in the structure of Nogo-66 in Fig. 1A. There are other groups conserved in higher vertebrates that appear to participate in intra-molecular helix–helix interactions (Arg1–Asp/Glu32, Leu65) or modulate secondary structure (Gly16, Pro18). These may play a role in folding the RHD-66 but do not appear to interact directly with lipid based on our previous study of accessibility and NOE contacts to DPC.

Inspection of the Nogo-66/DPC structure reveals that the hyperconserved Glu26 side chain is positioned at the base of a cavity and it is not involved in any interactions with charged functional groups from the protein that could neutralize the carboxylate. A model of PC binding in the Glu26 cavity shows that the choline group fits very well (Fig. 2A). In fact, NOEs were previously found between protein groups and the DPC headgroup (Fig. 2B). Other examples of PC-protein binding are shown in Fig. 2C–E. Since it appears plausible that the Glu26 cavity in Nogo-66 could similarly bind PC, we hypothesized that Glu26 could play a role in the determining the protein structure; we tested this by mutation of Glu26 to Ala, a group unable to bind choline through ionic interactions.

3.1. Secondary structure and partitioning of E26A into the lipid phase

The structural features of Nogo-66 wild type (WT) have been described by circular dichroism (CD) and NMR spectroscopies [20]. These experiments were performed in the aqueous phase where functional assays have shown Nogo-66 is active as an axonal growth inhibitor, and in the presence of lipid or detergent. We mutated Glu26 to alanine and compared CD spectra of this sample to Nogo-66 WT in both the aqueous phase and in the presence of DMPC lipid vesicles. We assessed the secondary structure of E26A using CD in Fig. 3A. The CD spectrum of Nogo-66 WT in water features little helical content (15%) and a substantial contribution of random coil below 205 nm. In contrast, the CD spectrum of the mutant E26A shows a canonical helical signature, estimated to be 38% helix (Fig. 3A blue). Previously, we demonstrated that addition of lipid vesicles to Nogo-66 WT induces a dramatic increase in helical content (to 85% helix) [20]. We performed a similar measurement for E26A but found a more modest increase in helical content when lipid was added, E26A is estimated to be 64% helical in DMPC. Based on these CD data, E26A is ~23% more helical in water but ~21% less structured in the presence of lipid compared to WT; transfer of E26A into the lipid phase only increases the helical content by ~16%.

Since the lipid bilayer is a liquid phase, the partition coefficient, K_X is the correct term to compare the affinities of Nogo-66 WT and E26A with the lipid phase [23]. This can be calculated from a change in ellipticity (θ, mdeg) if a peptide or protein shows substantial folding in the presence of lipid. We measured CD spectra of WT and E26A with increasing DMPC lipid concentration and normalized the change in ellipticity at 222 nm between the two samples to determine the fraction of protein (f_p) partitioned into lipid. Fig. 3B shows the partitioning of E26A compared to WT. Notably, the two proteins transfer favorably into the lipid phase with very similar partition coefficients (WT: $K_X = 1.8 \times 10^5$; E26A: $K_X = 1.2 \times 10^5$). The corresponding free energies of transfer are virtually identical: $\Delta G = -5.8$ kcal/mol for WT and $\Delta G = -5.6$ kcal/mol for E26A.

3.2. NMR characterization of E26A

We prepared a ^{15}N-labeled sample of Nogo-66 E26A and collected ^{15}N-HSQC NMR spectra as a measure of tertiary structure. Although CD data described above indicate that E26A is more helical in an

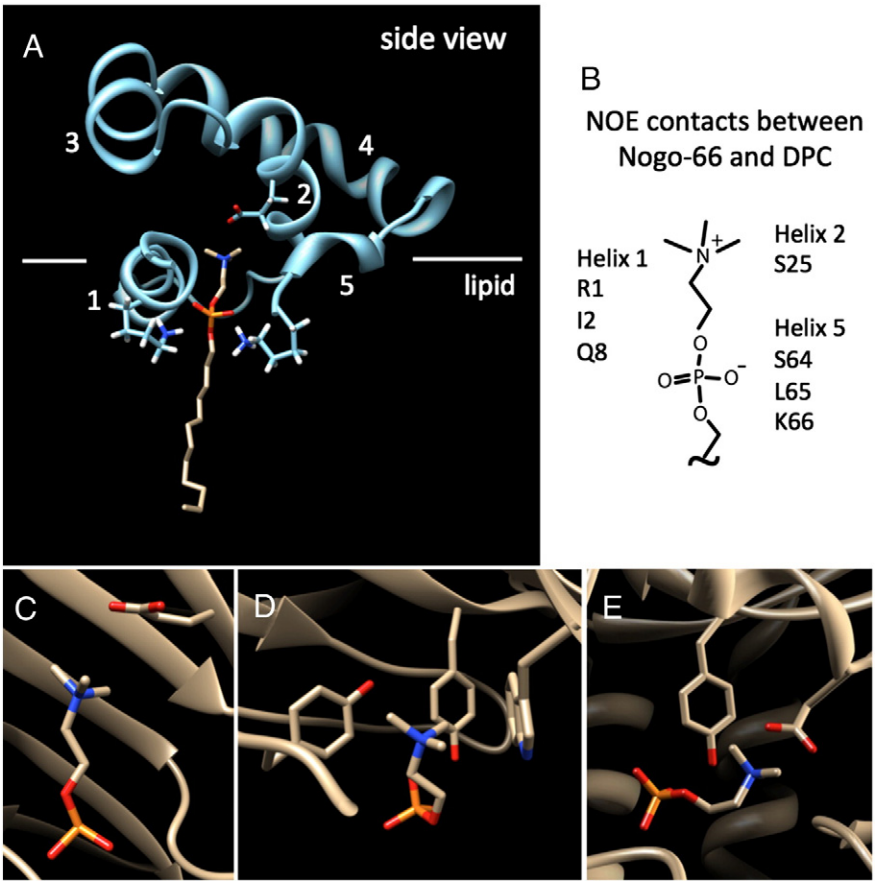

Fig. 2. A) Model of a single DPC molecule docked into the Nogo-66 Glu26 cavity by manually adjusting the position of DPC and cationic side chains. Helices 1–5 are numbered. B) NOEs previously determined between protein and DPC guide placement of the DPC phosphocholine in contact with helices 1 and 5 and in proximity to Glu26 [20]. Several other proteins are known to bind the choline cation of a phosphocholine group via interaction with either a Glu or Asp carboxylate and/or aromatic π–cation bonding. C) Human C-reactive protein (PDB ID: 1B09) binds a PC at the protein surface through ionic interactions forming a salt bridge between choline and Glu81. D) The antibody MC/Pc603 Fab–PC complex (PDB ID: 2MCP) binds the choline using aromatic ring π–cation interactions. E) The enzyme PfPMT (PDB ID: 3UJC) produces PC as a product. In this case, the protein binds choline using both π–cation and ionic interactions.

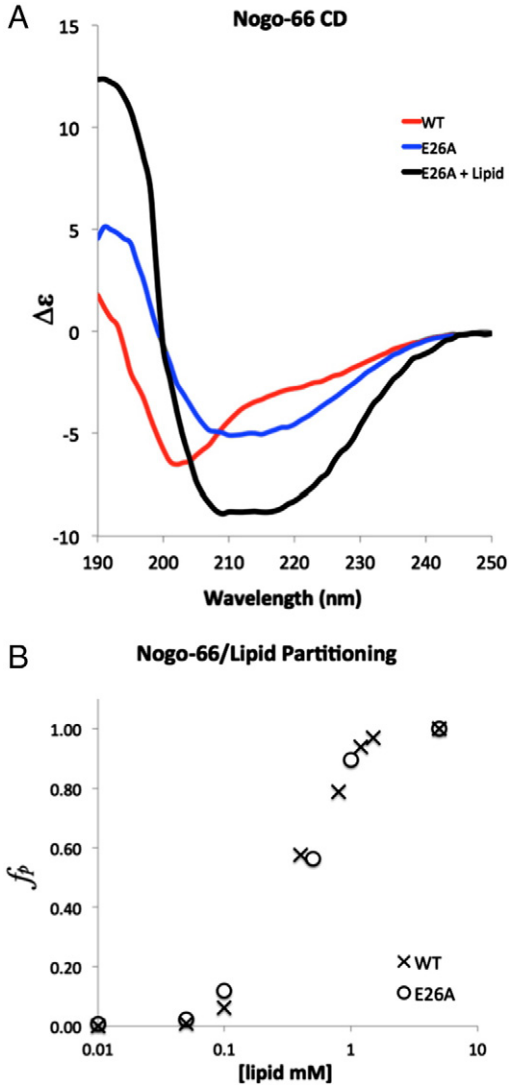

Fig. 3. Secondary structure and lipid partitioning of WT and E26A Nogo-66 determined by CD spectroscopy. A) Comparison of CD spectra of WT (red) and E26A (blue) in an aqueous environment (5 mM Na acetate, pH 5.0, 25 °C). An increase in helical content (signal at 222 nm) is visible in the mutant spectra, WT is approximately 15% helical; E26A is calculated to be 38%. Addition of DMPC lipid vesicles (100 nm diameter) to E26A resulted in a significant increase in helical secondary structure (64%), but less than the increase seen for WT (85%) [20]. B) A plot of the fraction of protein in the lipid phase (calculated as 1 − normalized $\theta_{222\ nm}$) with increasing lipid concentrations. The partition coefficient for E26A ($K_X = 1.2 \times 10^5$) is only slightly lower than that of WT ($K_X = 1.8 \times 10^5$).

aqueous environment compared to WT, we found no long range NOEs in NMR experiments performed on E26A in water (this is similar to the results of NMR experiments on WT in an aqueous environment [20]). In addition, the protein amide groups of E26A exchange immediately with D_2O, indicating a lack of stable structure. Previously, WT Nogo-66 was found to be highly ordered in DPC, giving one set of strong NMR signals with many long-range NOEs [20]. In contrast, the ^{15}N-HSQC spectra of E26A in DPC is disordered with broad signals in the random coil region (Fig. 4). The protein in DPC appears to be molten and we find only a few NOEs in the E26A NOESY spectrum. Although Nogo-66 WT samples remained soluble for weeks at low pH, the E26A mutant is prone to aggregation under the same conditions. Comparison of NMR spectra for WT and E26A show a dramatic change in structure; the mutant spectra reveal conformational heterogeneity for this species.

3.3. Nogo receptor binding

Functional assays have largely been performed on Nogo-66 in the aqueous phase. Although Nogo-66 is disordered in water, it is active in blocking neuronal outgrowth. It is possible that Nogo-66 folds into a helical bundle on the receptor surface with a conformation similar to that of the lipid-bound state. Since E26A was found to stabilize a helical conformation for Nogo-66 (Fig. 3A), we chose to assess receptor binding for this mutant under conditions similar to functional assays (aqueous phase). The use of phage display has proven a sensitive indicator of Nogo-66 binding to the receptor [16]. Nogo-66 and the NgR are not soluble at the same pH; this presents a challenge for binding assays. We have determined that the NgR is unfolded at the pH optimal for Nogo-66 solubility (pH 4) and Nogo-66 begins to precipitate above pH 5 where the receptor is stable. Phage display is a powerful technique in determining binding of a large library of mutant proteins in a single measurement. Display of the protein Nogo-66 on a phage particle offers another significant advantage: the phage particle is an enormous solubility tag. Phage can be concentrated to a point where they form liquid crystals and still remain soluble. Expression of Nogo-66 on the phage surface keeps Nogo-66 in solution and monodisperse, allowing for robust binding assays.

Monotopic membrane proteins, like Nogo-66, can be displayed consistently using a mutant helper phage, termed M13-KO7$^+$ or KO7$^+$, to package the phage. KO7$^+$ incorporates an extra positively-charged functionality into the phage coat, which can better mimic the zwitterionic composition of phospholipid head groups [26]. In the experiments reported here, Nogo-66 is displayed as a fusion to the major coat protein, P8 on the surface of KO7$^+$ packaged phage particles. A FLAG epitope fused to the N-terminus allows estimation of relative levels of the displayed proteins.

After successful mutagenesis of the Nogo-66 WT phagemid to incorporate the E26A point mutation, a phage-based ELISA confirmed the display of the Nogo-66 E26A variant. In this assay, an anti-FLAG antibody was immobilized on a 96-well microtiter plate. Subsequent to the wells being blocked with BSA, Nogo-66 E26A-displayed phage was incubated with the anti-FLAG antibody. The wells were washed to remove any unbound phage. Anti-M13 antibody specific to the phage was then incubated, and the relative levels of displayed Nogo-66 WT and E26A variant were measured by HRP activity (supplemental information, Fig. S1). Following confirmation of the successful display of the Nogo-66 variant, the binding of the phage-displayed Nogo-66 E26A to NgR was examined (Fig. S1). In order to determine the relative binding affinity of the Nogo-66 variant from the absorbance levels, the display levels and binding levels were measured on the same ELISA plate (Figs. 5 and S1). Negative controls included binding to NgR by KO7$^+$ phage without Nogo-66 displayed and binding of phage-displayed Nogo-66, wild-type and variant to the blocking agent, BSA; as expected, the negative controls for the Nogo-66 variants displayed essentially no binding (Fig. S1).

As shown previously [27], the ratio of the Nogo-66 binding levels (A) to display levels (A^0) has a linear correlation to the K_A for the interaction, provided the concentration of the target protein (NgR) greatly exceeds the concentration of the displayed protein. This is a reasonable assumption for a phage-displayed 7.5 kD protein. Thus, a correlation likely exists between the apparent and actual K_A of the NgR binding to Nogo66 wild-type and the variant. The binding affinity as apparent K_A of the Nogo-66 E26A relative to wild-type is represented in Fig. 5. The mutation of Glu26 to Ala resulted in a four-fold increase in affinity to the receptor.

4. Discussion

Many proteins that act at the membrane interface would be expected to recognize and bind PC. Interactions between positively charged Arg and Lys side chains and the phosphate or other lipid anion have

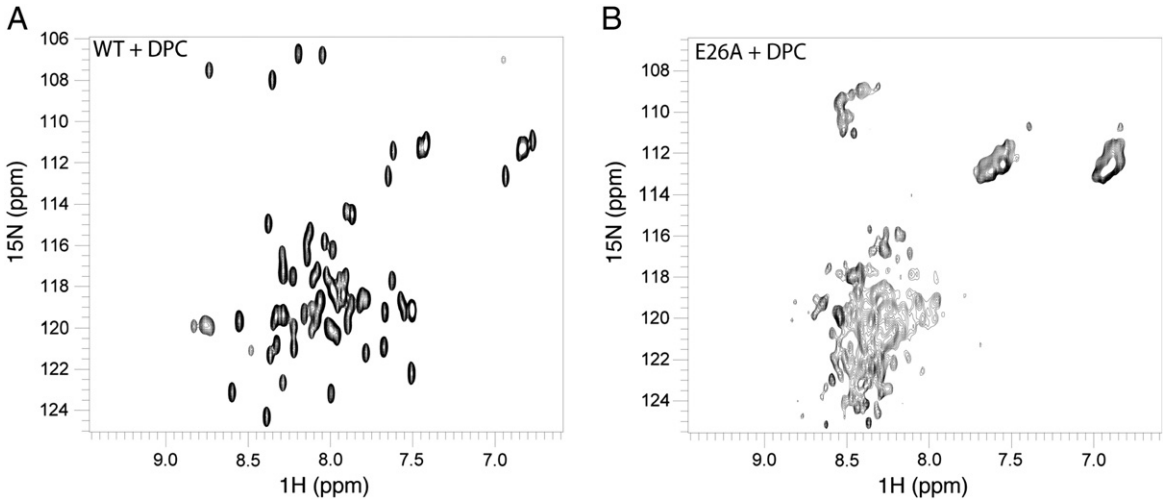

Fig. 4. Tertiary structure of WT and E26A Nogo-66 in DPC assessed by NMR spectroscopy. 800 MHz ^{15}N HSQC spectra of A) WT and B) E26A Nogo-66 in 200 mM DPC.

been studied in detail, most notably for antimicrobial peptides. However, choline binding has been less characterized. Protein crystal structures with good density describing the position of the PC reveal two major contributors to binding choline: aromatic π–cation interactions and Glu or Asp carboxylate-choline ionic interactions. The first structure showing a bound PC was an antibody determined by the Davies laboratory (Fig. 2D, [28]). In that structure, three aromatic residues Trp107, Tyr33, Tyr100 form a perfect pocket for the positively-charged choline group, highlighting π–cation binding. Human C-reactive protein (CRP) levels are elevated in response to acute infection, and it binds to PC on the surface of dead cells to initiate clearance. From the crystal structure of CRP, it is clear that the positively charged choline moiety of PC is in contact with the negatively charged Glu81 side chain, whereas the phosphate group interacts with protein-bound calcium (Fig. 2C, [29]). Another example of PC binding is seen in the structure of phosphoethanolamine methyltransferase from Plasmodium falciparum (PfPMT). In this case, a mixed π and anion pair: Tyr160 and Asp128, interact with choline to stabilize the PC enzyme product (Fig. 2E, [30]).

Although we previously performed NMR experiments of Nogo-66 in DPC, the NMR structure calculation relied only on NOE distance constraints between protein groups; no distance constraints to DPC molecules were included and the structure calculation was performed on the protein molecule alone (without lipid) [20]. Notably, the NOE constraints limited to protein–protein contacts created a cavity near Glu26 that can accommodate exactly one PC molecule in the Nogo-66 structure. Tyr22 is one helical turn from Glu26 and is positioned to π–cation bond with choline in Nogo-66 providing additional stabilization in PC docking; however, this Tyr is not conserved in all RHDs.

The results presented here show that structural influence of Glu26 depends on the environment of the protein — when either dissolved in an aqueous solvent or partially embedded at a PC surface. A summary of the structural features present under each condition is shown in Fig. 6. Both WT and E26A Nogo-66 have similar partition coefficients (K_X) of transfer from water into the lipid phase, but dramatically different structures on a PC surface. WT folds into a single conformer in DPC but E26A, unable to form a stable salt bridge to choline, is disordered

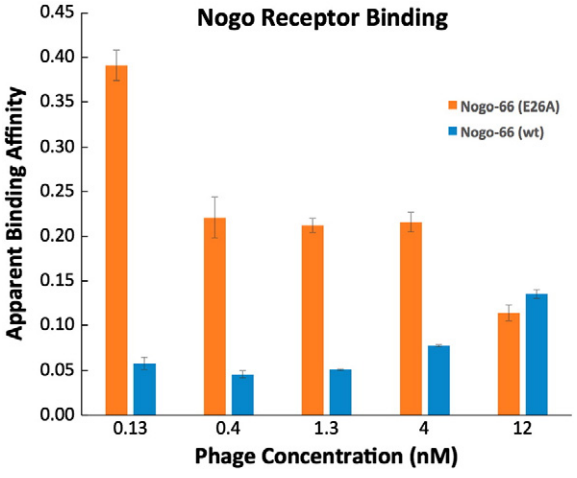

Fig. 5. Apparent binding affinity of Nogo-66 WT and E26A mutant to the Nogo receptor. The apparent binding affinity is calculated as the apparent K_A of the ligand–receptor interaction. The apparent K_A is determined as the ratio of the binding levels of the protein (Nogo-66 WT or E26A) with its target (NgR) (A) to the amount of displayed protein (Nogo-66 WT or E26A) on the phage surface (A^0) [27]. A single microtiter plate was used to simultaneously measure display levels and binding levels of Nogo-66 WT and E26A mutant. Each concentration was in triplicate and the average plotted. Standard errors are shown. In the range where the apparent K_A is linear, the mutant E26A shows a binding affinity for NgR that is four-fold higher than that of WT.

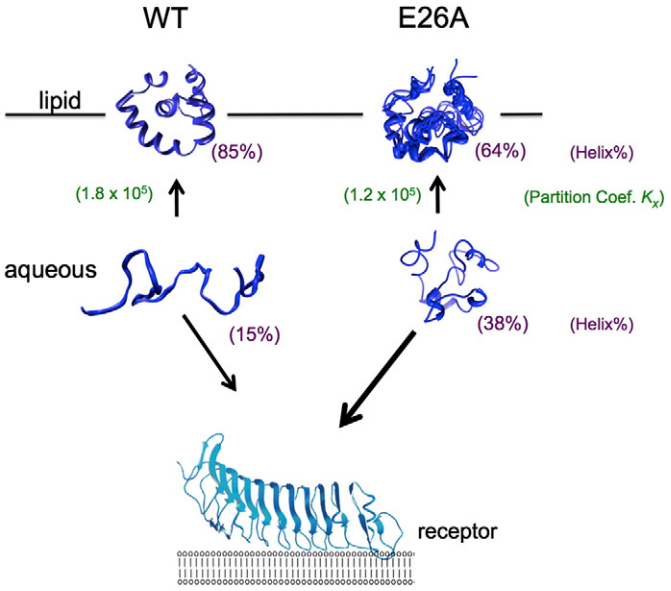

Fig. 6. Summary of the effect of Glu26 mutation in Nogo-66. Although both proteins are strongly associated with lipid, E26A is more disordered than WT. In contrast, E26A is more helical in the aqueous phase than WT and binds the receptor with higher affinity.

and less helical. The similarity in transfer energy between WT and mutant when partitioning into lipid could be accounted for by compensating effects; an energetically favorable increase in entropy of disordered E26A in DPC could compensate for the destabilization resulting from a lost salt bridge between Glu and the lipid headgroup.

In an aqueous environment, Nogo-66 WT is active in functional assays but maintains a very disordered structure. In contrast, mutation of the buried Glu26 charge to Ala stabilizes helical conformations and increases helical content by ~23% in E26A. Moreover, Nogo-66 E26A has a much higher affinity for the receptor than WT in an aqueous environment; this effect is most likely a consequence of stabilized secondary structure in the lipid-free state. Although a complete structure of the complex between NgR, Nogo-66 and lipid has not been determined, these studies provide insight into the state of Nogo-66 when binding the receptor. We observe that the interaction of Glu26 with lipid stabilizes the WT protein fold. In contrast, when lipid is absent Glu26 destabilizes both the helical fold and receptor binding. The region 31–55 is known to contain residues sufficient for Nogo-66 function; Glu26 is positioned on the opposite protein face compared to the functional groups. The ability of a position within the interior of a compact helical bundle (Glu26) to affect receptor binding when it is not among the residues expected to make up the binding interface suggests a model where Nogo-66 folds on the receptor into a structure similar to that induced by lipid.

The RHD-66 domain is flanked by two membrane-embedded helices that are believed to induce curvature of the ER membrane. These structures would be expected to stabilize the RHD-66 structure, both in anchoring the protein to the membrane and in extending the N- and C-terminal helices. It is also expected that the RHD-66 would be more stable in a natural membrane than in DPC micelles. Compared to planar bilayers, micelles are highly curved and much more dynamic. It is possible that the loss in structure seen in the lipid-associated state for the E26A mutant is not as pronounced in the context of the full-length protein and natural cell membranes. Nevertheless, a system that is on the cusp of stability is actually very useful in understanding protein folding. Proteins that are extremely stable will often not show a measurable effect from a single mutation; this can make it difficult to determine the relative contributions of individual amino acids to the overall protein stability. In deconstructing the RHD, we have found that Nogo-66 is an excellent model for testing the forces that drive protein folding at a lipid interface as well as providing specific detail on the RHD-66 fold. The structure of Nogo-66 in DPC is entirely consistent with functional assays and these studies show that Nogo-66 is an autonomous folding unit that uses a negative charge at position 26 to anchor the protein to the membrane surface. Nearby aromatic rings can also anchor Nogo-66 in the membrane and contribute to the lipid-induced fold. In addition, there are several other Glu/Asp side chains conserved in higher vertebrates that could interact with choline and drive docking into the membrane leaflet. Studies are ongoing to extend the structure of Nogo-66 with the flanking membrane embedded regions and define a complete RHD structure.

Acknowledgements

We thank Jessica Schulz for sub-cloning the NgR gene, and Deepthi Tummala for assisting in the preparation of Nogo receptor. We are grateful to Sudipta Majumdar for expert advice and assistance on the receptor binding experiments and to Antje Pokorny for the stimulating conversation and advice on phosphocholine–protein interactions. We thank Sean Moro for critically reading this manuscript. This work was supported by the National Institutes of Health (GM069783), National Institute of General Medical Sciences (R01-GM078528-0, R01-GM069783-06 and R01 GM100700-01), the Roman Reed Research Fund (RR05-155) and the Ministry of Higher Education, King Saud University, Riyadh, Saudi Arabia.

Appendix A. Supplementary data

Supplementary data to this article can be found online at http://dx.doi.org/10.1016/j.bbamem.2014.05.021.

References

[1] T. Oertle, M. Klinger, C.A. Stuermer, M.E. Schwab, A reticular rhapsody: phylogenic evolution and nomenclature of the RTN/Nogo gene family, FASEB J. 17 (2003) 1238–1247.
[2] G.K. Voeltz, W.A. Prinz, Y. Shibata, J.M. Rist, T.A. Rapoport, A class of membrane proteins shaping the tubular endoplasmic reticulum, Cell 124 (2006) 573–586.
[3] E. Kiseleva, K.N. Morozova, G.K. Voeltz, T.D. Allen, M.W. Goldberg, Reticulon 4a/NogoA locates to regions of high membrane curvature and may have a role in nuclear envelope growth, J. Struct. Biol. 160 (2007) 224–235.
[4] Y.S. Yang, S.M. Strittmatter, The reticulons: a family of proteins with diverse functions, Genome Biol. 8 (2007) 234.
[5] A. Diaz, P. Ahlquist, Role of host reticulon proteins in rearranging membranes for positive-strand RNA virus replication, Curr. Opin. Microbiol. 15 (2012) 519–524.
[6] S. Tagami, Y. Eguchi, N. Kinoshita, Y. Takeda, Y. Tsujimoto, A novel protein, RTN-XS, interacts with both Bcl-XL and Bcl-2 on endoplasmic reticulum and reduces their anti-apoptotic activity, Oncogene 19 (2000) 5736–5746.
[7] L. Zhu, R. Xiang, W. Dong, Y.L. Liu, Y.P. Qi, Anti-apoptotic activity of Bcl-2 is enhanced by its interaction with RTN3, Cell Biol. Int. 31 (2007) 825–830.
[8] W. He, Y. Lu, I. Qahwash, X.Y. Hu, A. Chang, R. Yan, Reticulon family members modulate BACE1 activity and amyloid-beta peptide generation, Nat. Med. 10 (2004) 959–965.
[9] W. He, Q. Shi, X. Hu, R. Yan, The membrane topology of RTN3 and its effect on binding of RTN3 to BACE1, J. Biol. Chem. 282 (2007) 29144–29151.
[10] L. Acevedo, J. Yu, H. Erdjument-Bromage, R.Q. Miao, J.E. Kim, D. Fulton, P. Tempst, S. M. Strittmatter, W.C. Sessa, A new role for Nogo as a regulator of vascular remodeling, Nat. Med. 10 (2004) 382–388.
[11] T. Walchli, V. Pernet, O. Weinmann, J.Y. Shiu, A. Guzik-Kornacka, G. Decrey, D. Yuksel, H. Schneider, J. Vogel, D.E. Ingber, V. Vogel, K. Frei, M.E. Schwab, Nogo-A is a negative regulator of CNS angiogenesis, Proc. Natl. Acad. Sci. U. S. A. 110 (2013) E1943–E1952.
[12] S.Y. Chong, S.S. Rosenberg, S.P. Fancy, C. Zhao, Y.A. Shen, A.T. Hahn, A.W. McGee, X. Xu, B. Zheng, L.I. Zhang, D.H. Rowitch, R.J. Franklin, Q.R. Lu, J.R. Chan, Neurite outgrowth inhibitor Nogo-A establishes spatial segregation and extent of oligodendrocyte myelination, Proc. Natl. Acad. Sci. U. S. A. 109 (2011) 1299–1304.
[13] V. Pernet, M.E. Schwab, The role of Nogo-A in axonal plasticity, regrowth and repair, Cell Tissue Res. 349 (2012) 97–104.
[14] A. Schmandke, A. Schmandke, M.E. Schwab, Nogo-A: multiple roles in CNS development, maintenance, and disease, Neuroscientist (2014), http://dx.doi.org/10.1177/1073858413516800 PMID: 24402613.
[15] F. Di Sano, P. Bernardoni, M. Piacentini, The reticulons: guardians of the structure and function of the endoplasmic reticulum, Exp. Cell Res. 318 (2012) 1201–1207.
[16] M.S. Chen, A.B. Huber, M.E. van der Haar, M. Frank, L. Schnell, A.A. Spillmann, F. Christ, M.E. Schwab, Nogo-A is a myelin-associated neurite outgrowth inhibitor and an antigen for monoclonal antibody IN-1, Nature 403 (2000) 434–439.
[17] T. GrandPre, F. Nakamura, T. Vartanian, S.M. Strittmatter, Identification of the Nogo inhibitor of axon regeneration as a reticulon protein, Nature 403 (2000) 439–444.
[18] R. Prinjha, S.E. Moore, M. Vinson, S. Blake, R. Morrow, G. Christie, D. Michalovich, D.L. Simmons, F.S. Walsh, Inhibitor of neurite outgrowth in humans, Nature 403 (2000) 383–384.
[19] A.E. Fournier, T. GrandPre, S.M. Strittmatter, Identification of a receptor mediating Nogo-66 inhibition of axonal regeneration, Nature 409 (2001) 341–346.
[20] S.V. Vasudevan, J. Schulz, C. Zhou, M.J. Cocco, Protein folding at the membrane interface, the structure of Nogo-66 requires interactions with a phosphocholine surface, Proc. Natl. Acad. Sci. U. S. A. 107 (2010) 6847–6851.
[21] L. Whitmore, B.A. Wallace, DICHROWEB, an online server for protein secondary structure analyses from circular dichroism spectroscopic data, Nucleic Acids Res. 32 (2004) W668–W673.
[22] J.G. Lees, A.J. Miles, R.W. Janes, B.A. Wallace, Novel methods for secondary structure determination using low wavelength (VUV) circular dichroism spectroscopic data, BMC Bioinforma. 7 (2006) 507.
[23] S.H. White, W.C. Wimley, A.S. Ladokhin, K. Hristova, Protein folding in membranes: determining energetics of peptide-bilayer interactions, Methods Enzymol. 295 (1998) 62–87.
[24] F. Delaglio, S. Grzesiek, G.W. Vuister, G. Zhu, J. Pfeifer, A. Bax, NMRPipe: a multidimensional spectral processing system based on UNIX pipes, J. Biomol. NMR 6 (1995) 277–293.
[25] X.L. He, J.F. Bazan, G. McDermott, J.B. Park, K. Wang, M. Tessier-Lavigne, Z. He, K.C. Garcia, Structure of the Nogo receptor ectodomain: a recognition module implicated in myelin inhibition, Neuron 38 (2003) 177–185.
[26] R. Vithayathil, R.M. Hooy, M.J. Cocco, G.A. Weiss, The scope of phage display for membrane proteins, J. Mol. Biol. 414 (2011) 499–510.
[27] S. Rossenu, S. Leyman, D. Dewitte, D. Peelaers, V. Jonckheere, M. Van Troys, J. Vandekerckhove, C. Ampe, A phage display-based method for determination of relative affinities of mutants. Application of the actin-binding motifs in thymosin beta 4 and the villin headpiece, J. Biol. Chem. 278 (2003) 16642–16650.
[28] Y. Satow, G.H. Cohen, E.A. Padlan, D.R. Davies, Phosphocholine binding immunoglobulin Fab Mcpc603. An X-ray-diffraction study at 2.7 A, J. Mol. Biol. 190 (1986) 593–604.
[29] D. Thompson, M.B. Pepys, S.P. Wood, The physiological structure of human C-reactive protein and its complex with phosphocholine, Structure 7 (1999) 169–177.
[30] S.G. Lee, Y. Kim, T.D. Alpert, A. Nagata, J.M. Jez, Structure and reaction mechanism of phosphoethanolamine methyltransferase from the malaria parasite Plasmodium falciparum: an antiparasitic drug target, J. Biol. Chem. 287 (2012) 1426–1434.